APPLIED MATERIALS AND TECHNOLOGY

Jamt.ejournal.unri.ac.id

Research Article

Development, microstructural characterization, and photocatalytic evaluation of TiO_2-modified rendering mortars

Vander Alkmin dos Santos Ribeiro, Adhimar Flávio Oliveira*, Celso Henrique Correa Carvalho, Lucas Pacca e Silva

ABSTRACT: The growing demand for sustainable construction materials has spurred research into cement-based composites that can contribute to environmental remediation. In this context, photocatalytic materials containing titanium dioxide (TiO_2) have attracted considerable attention due to their ability to degrade organic pollutants under ultraviolet radiation. This study aimed to develop and evaluate TiO_2-modified rendering mortars with enhanced photocatalytic performance for potential application in building facades and surface coatings. Mortar mixtures were produced with 0%, 2%, 6%, and 10% TiO_2, expressed as a percentage of cement mass. The materials were characterized through ultraviolet–visible (UV–Vis) spectroscopy, scanning electron microscopy coupled with energy-dispersive spectroscopy (SEM/EDS), and X-ray diffraction (XRD). Photocatalytic activity was assessed using methylene blue degradation tests under UV irradiation. The results demonstrated that TiO_2 incorporation influenced the methylene blue removal behavior of the mortars under UV irradiation. Among the TiO_2-modified formulations, the mortar containing 10 wt.% TiO_2 exhibited the highest overall removal efficiency. Because no adsorption–desorption equilibrium was established before irradiation, the measured dye removal represents the combined effects of adsorption and photocatalytic degradation. Microstructural analyses confirmed the presence and distribution of TiO_2 particles within the cementitious matrix and indicated changes associated with increasing nanoparticle content. Although higher TiO_2 additions enhanced photocatalytic performance, they also reduced the workability of the fresh mortars. Overall, the findings demonstrate the potential of TiO_2-modified rendering mortars as multifunctional construction materials capable of combining conventional protective functions with photocatalytic properties for environmental remediation applications.

Keywords: *Titanium dioxide (TiO_2), Photocatalytic mortars, Rendering mortars, Methylene blue degradation, Environmental remediation*

1. INTRODUCTION

The increasing rate of urbanization and the intensification of human activities have generated significant environmental impacts, particularly through the rise of atmospheric pollution in urban centers. This issue not only compromises the population's quality of life but also highlights the need for innovative solutions to mitigate its effects. In the construction sector, one of the industries with the highest consumption of natural resources, the development of sustainable and technologically advanced materials has become a priority [1].

The characterization of rendering mortars with photocatalytic properties has gained considerable attention in recent decades due to their potential to reduce atmospheric pollution and promote more sustainable built environments. Rendering mortars are widely used in the construction industry, playing a fundamental role in the protection and finishing of surfaces. However, the continuous increase in urban pollution, combined with the search for innovative solutions that contribute to environmental quality, has encouraged the development of

OPEN ACCESS

Affiliation
Universidade Federal de Itajubá (UNIFEI), Av. BPS, 1303, Itajubá, Minas Gerais, 37500-903, Brazil.

***Correspondence**
Email: adhimarflavio@unifei.edu.br

ORCID
Vander Alkmin dos Santos Ribeiro: 0000-0003-0260-2454
Adhimar Flávio Oliveira: 0000-0003-2586-7359
Celso Henrique Correa Carvalho: 0000-0001-7667-6961
Lucas Pacca e Silva: 00009-0009-1097-0557

Received: June 15, 2026
Revised: July 6, 2026
Accepted: July 14, 2026

How to cite: Ribeiro, V. A dos S., Oliveira, A. F., Carvalho, C. H. C., e Silva, L. P., (2026). Development, microstructural characterization, and photocatalytic evaluation of TiO_2-modified rendering mortars. Journal of Applied Materials and Technology, 8(1), 41–54. https://doi. org/10.31258/Jamt.8.1.41-54.

construction materials with additional functional properties, such as photocatalytic activity [2]. Photocatalysis, which constitutes the fundamental mechanism of this type of mortar, refers to the ability of certain photocatalytic materials to promote chemical reactions in the presence of light, typically ultraviolet (UV) or visible radiation.

This phenomenon has been extensively investigated due to its applications in self-cleaning surfaces, air purification, and resistance to microbial growth [3]. When exposed to light, photocatalytic mortars can promote chemical reactions capable of degrading atmospheric pollutants, such as nitrogen oxides (NOx) and volatile organic compounds (VOCs), as well as decomposing organic substances deposited on their surfaces, thereby providing self-cleaning properties. Consequently, photocatalytic mortars represent a promising alternative for façades and exposed surfaces, combining functional performance, sustainability, and durability in modern construction systems [4].

An ideal photocatalyst for such applications should exhibit specific characteristics, including high optical activity, strong absorption capacity in the ultraviolet and visible light regions, an appropriate band-gap energy to facilitate chemical reactions, chemical inertness, optical stability, and low cost. Among the various materials available, titanium dioxide (TiO_2) stands out as one of the most efficient photocatalysts because of its high chemical stability, resistance to corrosion by most acids, bases, and organic solvents, as well as its economic viability.

Titanium dioxide exists in three crystalline polymorphs: anatase, rutile, and brookite. The anatase structure consists of TiO_6 octahedra sharing corners to form (001) planes, resulting in a tetragonal crystal structure (I41/amd). In rutile, the octahedra share edges within the (001) planes, leading to a tetragonal structure (P42/mnm), whereas brookite exhibits both edge-sharing and corner-sharing octahedra, resulting in an orthorhombic structure (Pbca). Among these polymorphs, anatase is the most widely used because of its superior photocatalytic activity compared with the other TiO_2 phases [5].

The band-gap energy of titanium dioxide in its most photocatalytically active form (anatase) is approximately 3.2 eV. Consequently, its photoabsorption properties are mainly associated with ultraviolet irradiation, corresponding to wavelengths below approximately 387 nm [6]. The photocatalytic activity of TiO_2 is intrinsically related to its semiconductor nature, which enables the generation of electron–hole pairs under ultraviolet irradiation. These charge carriers promote the formation of highly reactive oxygen species capable of oxidizing a wide range of organic pollutants, making TiO_2 one of the most extensively investigated photocatalysts for environmental remediation [6, 25, 36, 37].

However, ultraviolet radiation represents only a small fraction of the solar spectrum, whereas a significant proportion of solar photons lies within the visible region. As a result, photocatalytic processes driven solely by UV radiation may exhibit limited efficiency under natural sunlight conditions. Therefore, considerable research efforts have been devoted to modifying TiO_2 in order to extend its light absorption capability into the visible spectrum and enhance its photocatalytic performance under solar irradiation [7].

Due to these properties, TiO_2 has found extensive application in the construction industry, particularly in photocatalytic rendering mortars [4]. Nevertheless, an important gap remains in the literature regarding the evaluation of the performance of photocatalytic mortars under real service conditions. Studies investigating the implementation of these materials on building façades located in urban environments are essential to validate their effectiveness and support their large-scale adoption [8].

Although TiO_2-modified cementitious materials have been extensively investigated, most previous studies have focused on cement pastes, concrete, or mortars emphasizing either photocatalytic performance or isolated material properties. Comparatively fewer studies have systematically investigated rendering mortars by correlating TiO_2 content with mineralogical composition, microstructural characteristics, and photocatalytic behavior under identical experimental conditions. Furthermore, the influence of TiO_2 dosage on particle dispersion, phase composition, and photocatalytic efficiency remains insufficiently understood, particularly for rendering mortars intended for façade applications.

In this context, the present study aims to develop TiO_2-modified rendering mortars and to provide an integrated evaluation of their performance by combining X-ray diffraction (XRD), scanning electron microscopy coupled with energy-dispersive spectroscopy (SEM/EDS), and photocatalytic degradation tests using methylene blue under UV irradiation. By correlating microstructural features with photocatalytic performance, this work contributes to a better understanding of the mechanisms governing the behavior of photocatalytic rendering mortars and supports their potential application as multifunctional building materials for environmental remediation.

2. MATERIALS AND METHODS

2.1. Materials. The following materials were used to produce the photocatalytic rendering mortars: natural washed sand as fine aggregate; titanium dioxide (TiO_2) supplied by VETEC (Sigma-Aldrich Brazil Ltda.); CH-III hydrated lime (Monte Branco), complying with ABNT NBR 7175 (2003) [9]; CP II-E 32 Portland cement (CSN), complying with ABNT NBR 16697 (2018) [10]; and potable water for mixing.

The specific gravity of the fine aggregate was determined according to ABNT NBR 16916 (2021) [11]. A value of 1.66 g/cm^3 was obtained, meeting the requirements established by the standard for aggregate characterization.

The specific gravity of Portland cement was determined following ABNT NBR 16605 (2017) [12], which prescribes a method based on the use of a volumetric flask, such as the Le Chatelier flask. The measured specific gravity was 2.80 g/cm^3, satisfying the requirements for Portland cement characterization.

2.2. Mortar preparations. A volumetric mix proportion of 1:2:8 (cement lime) was adopted for the production of the rendering mortars. Different concentrations of titanium dioxide (TiO_2) were incorporated into the mixtures, corresponding to 0% (reference mixture), 2%, 6%, and 10% by mass of cement.

The materials were thoroughly mixed to ensure homogeneous dispersion of TiO_2 throughout the mortar matrix. The quantities of materials used for specimen preparation and the corresponding water-to-cement (w/c) ratio, adjusted to achieve the consistency recommended by the applicable standards, are presented in Table 1. The mixtures were molded into specimens measuring 5 cm × 5 cm × 1 cm

Table 1. Material consumption and water-to-cement ratio of the mortar mixtures.

TiO_2 (%)	Cement (g)	Hydrated Lime (g)	Sand (g)	Water (mL)	TiO_2 (%)	w/c ratio
0	4.09	8.18	32.73	2.05	0.00	0.5
2	4.09	8.18	32.73	2.05	0.08	0.5
6	4.09	8.18	32.73	2.05	0.25	0.5
10	4.09	8.18	32.73	2.05	0.41	0.5

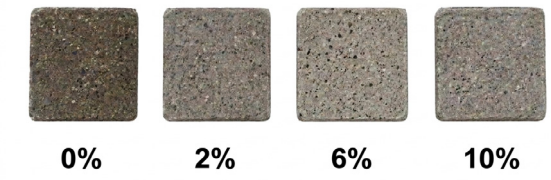

Figure 1. Mortar specimens (5 cm × 5 cm × 1 cm) prepared for photocatalytic activity evaluation by UV–Vis spectrophotometry.

for photocatalytic evaluation using UV–Vis spectrophotometry, as illustrated in Figure 1.

2.3. Curing procedures. After casting, the specimens were subjected to moist curing for 28 days to ensure adequate hydration and full development of the mortar properties, as shown in Figure 2. The curing procedure was based on the recommendations of ABNT NBR 13279 (1995) [13] and ABNT NBR 13749 (2013) [14]. Although these standards are not specifically intended for photocatalytic materials, the curing period of 28 days is widely adopted to ensure the stabilization and maturation of cement-based materials. Following curing, the specimens were dried at room temperature to remove residual moisture before photocatalytic, X-ray diffraction (XRD), and scanning electron microscopy (SEM) analyses.

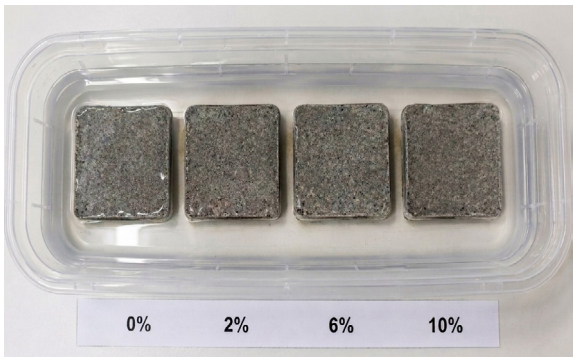

Figure 2. Mortar specimens were subjected to 28 days of moist curing before photocatalytic, microstructural, and mineralogical characterization.

2.4. Photocatalytic activity test. The photocatalytic performance of the mortars was evaluated using a K37-UV-VIS spectrophotometer (Kasvi). The test consisted of monitoring the degradation of methylene blue solution under controlled conditions. Initially, a methylene blue solution was prepared using distilled water at a concentration of 0.005 $g{\cdot}L^{-1}$, as shown in Figure 3.

The photocatalytic test was conducted by exposing the mortar–solution system to ultraviolet radiation while monitoring the degradation of the dye over time. Methylene blue was selected as a model organic pollutant commonly employed in photocatalytic studies due to its well-defined absorption characteristics and ease of quantification by UV–Vis spectroscopy. The absorbance measurements were performed under the experimental conditions described in Figure 3.

Using the absorbance curves and the linear fit obtained from reference standards, the methylene blue (MB) concentration in solution was quantitatively determined. This quantification enabled the evaluation of two key parameters for all reactors: degradation efficiency (DE) and degradation kinetics (k) [15-17]. Degradation efficiency (DE) quantifies the fraction of contaminant removed from the solution during the degradation process, where higher DE values indicate a more effective process. Degradation efficiency was calculated according to Equation (1):

$$DE(\%) = \frac{C_i - C_t}{C_i} x100 \qquad (1)$$

Where C_0 represents the initial dye concentration in solution, expressed in mol L^{-1} or g L^{-1}, and C_t denotes the contaminant con-centration at a given time t during the degradation process. Degradation kinetics is also an important parameter for under-standing how the contaminant degradation evolves. In this study, the degradation kinetics were described using a first-order kinetic model, expressed by Equation (2):

$$ln\left(\frac{C_i}{C_t}\right) = kt \qquad (2)$$

Where k is the apparent first-order rate constant, expressed in h^{-1}, and t is the irradiation or reaction time.

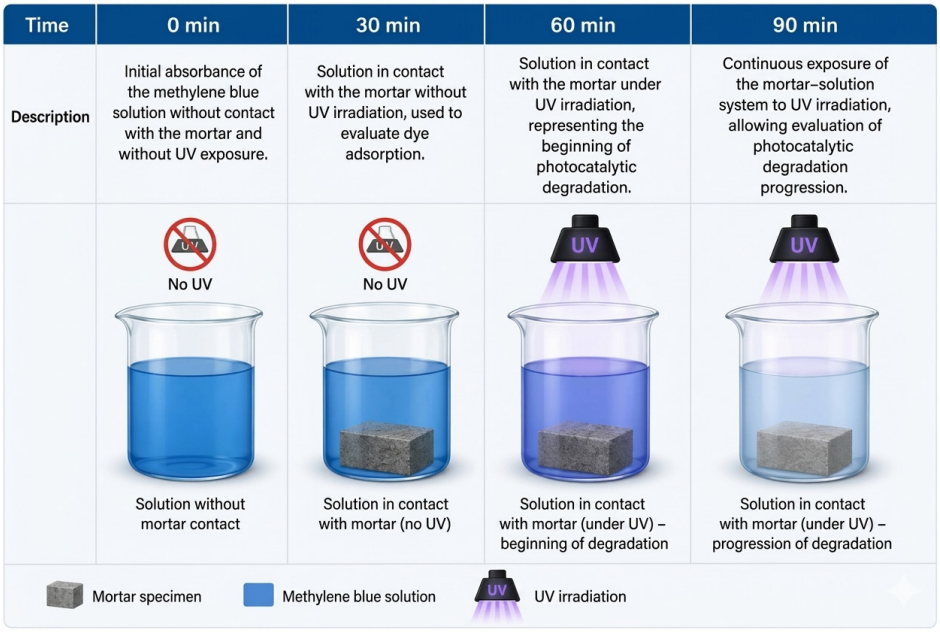

Figure 3. Experimental conditions adopted during the photocatalytic test.

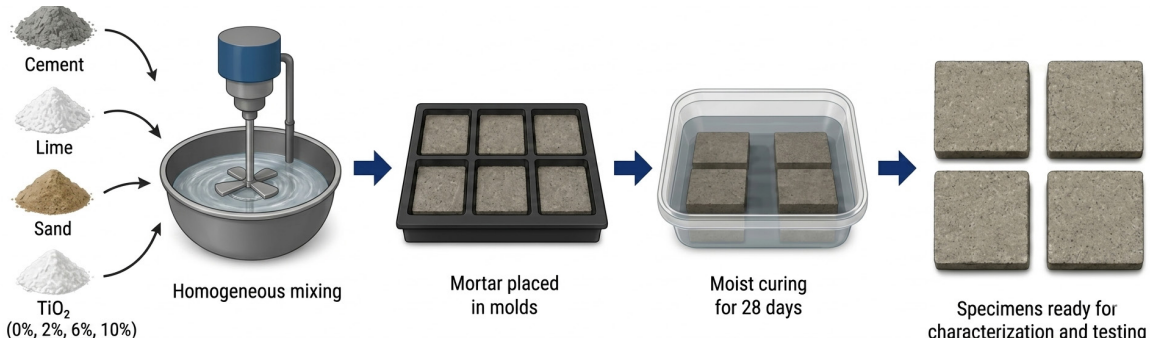

Figure 4. Shows the diagram, which provides a clear and reproducible overview of the experimental procedure.

2.5. Microstructural and mineralogical characterization. For X-ray diffraction (XRD) and scanning electron microscopy (SEM) analyses, the specimens were manually ground using an agate mortar and pestle until a fine and homogeneous powder was obtained. SEM images were acquired at different magnifications to evaluate the surface morphology, particle distribution, and possible TiO_2 agglomerates. Energy-dispersive spectroscopy (EDS) was performed for qualitative elemental analysis and to assess the incorporation of TiO_2 within the mortar matrix.

The crystalline phases present in the materials were identified by X-ray diffraction (XRD). The analyses were performed using a Philips X'Pert MPD diffractometer operating at 40 kV and 40 mA with CuKα radiation. Data were collected over a 2θ range from 5° to 80°, using a step size of 0.02° and a counting time of 1 s per step.

Phase identification was carried out using X'Pert HighScore software and reference patterns from the International Centre for Diffraction Data (ICDD) database. Figure 4 shows a diagram that provides a clear and reproducible overview of the experimental procedure.

3. RESULTS AND DISCUSSION

3.1. Particle size distribution of fine aggregate. Table 2 presents the particle size distribution of the fine aggregate used in the production of the photocatalytic rendering mortars. The obtained fineness modulus (FM) was 1.86, which classifies the material as fine sand according to ABNT NBR 7211 (2022) [18].

The maximum aggregate size was determined to be 0.60 mm, indicating a predominance of fine particles within the aggregate composition. The fine grading of the aggregate is expected to influence both the fresh and hardened properties of the mortars. Due to the higher specific surface area associated with finer particles, an increase in water demand and a reduction in workability may occur. This effect becomes particularly relevant in TiO_2-modified mortars, since the incorporation of photocatalytic particles further increases the overall surface area of the solid constituents.

In addition, the predominance of fine particles may contribute to improved packing density and greater homogeneity of the cementitious matrix, favoring a more uniform distribution of TiO_2

Table 2. Particle size distribution of the fine aggregate.

#Sieve Size (mm)	Mass Retained (g)	% Retained	% cumulative Retained	% Cumulative Passing
6.30	0.04	0.00	0.00	100.00
4.80	0.11	0.01	0.01	99.99
2.40	0.17	0.02	0.03	99.98
1.20	0.06	0.01	0.03	99.99
0.60	15.83	1.58	1.61	98.42
0.30	846.15	84.32	85.94	15.68
0.15	125.17	12.47	98.41	87.53
0.075	14.53	1.45	99.86	98.55
Pan	1.39	0.14	100.00	99.86
Σ	1003.45	100.00	-	0.00
Aggregate Specific Gravity(g/cm^3)	1.66	Fineness modulus		1.86
		Maximum aggregate size (mm)		0.60

throughout the mortar. Such characteristics are important because the photocatalytic efficiency of cement-based materials depends not only on the amount of TiO_2 incorporated but also on its dispersion and accessibility at the exposed surface.

The particle size distribution may also affect the microstructural characteristics observed in the SEM analyses, influencing pore distribution, particle arrangement, and the interaction between TiO_2 particles and hydration products. Therefore, the aggregate grading adopted in this study provides suitable conditions for evaluating the influence of TiO_2 incorporation on the photocatalytic performance and microstructural development of rendering mortars.

Figure 5 shows the particle size distribution curve of the fine aggregate. The continuous grading observed confirms the predominance of fine particles and supports the classification obtained from the fineness modulus.

The particle size distribution results indicated negligible cumulative retention in the sieve range from 6.3 mm to 1.20 mm, demonstrating the absence of coarse particles in the aggregate. This behavior confirms the predominance of fine particles, which is consistent with the fineness modulus value of 1.86 and the classification of the material as fine sand according to ABNT NBR 7211 (2022)[18].

A significant concentration of particles was observed between the 0.60 mm and 0.30 mm sieves, with the highest retention occurring at the 0.30 mm sieve. The particle size distribution curve remained within the acceptable limits established by the standard, indicating adequate grading for mortar production. The predominance of fine particles is advantageous for rendering mortars because it contributes to improved cohesiveness, reduced segregation, and enhanced surface finishing. Furthermore, the finer grading increases the specific surface area of the aggregate, which may influence the interaction between the cementitious matrix and the incorporated photocatalyst. For TiO_2-modified mortars, the presence of fine particles can facilitate a more homogeneous

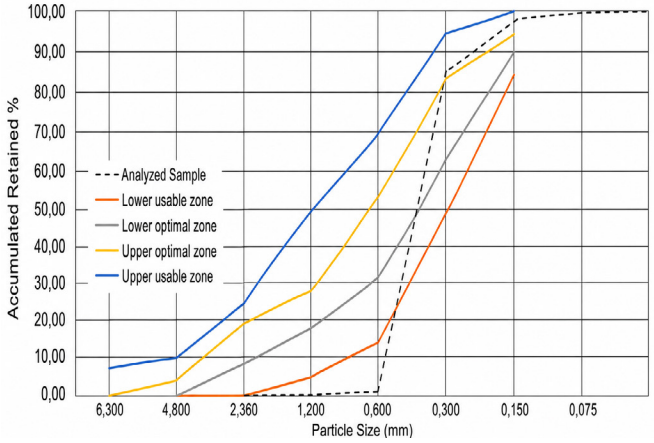

Figure 5. Particle size distribution curve of the fine aggregate.

distribution of the photocatalyst throughout the matrix, promoting greater exposure of active photocatalytic sites at the mortar surface. This characteristic is particularly important because photocatalytic efficiency depends not only on the amount of TiO_2 incorporated but also on its accessibility to ultraviolet radiation and pollutant molecules [19].

The high proportion of fine particles may also contribute to a denser microstructure by improving particle packing, which can affect pore distribution and the interaction between hydration products and TiO_2 particles. These effects are relevant for understanding the microstructural characteristics observed in the SEM analyses and the photocatalytic performance discussed in subsequent sections.

During mortar production, the incorporation of TiO_2 at replacement levels ranging from 2% to 10%, while maintaining the initial water content constant, resulted in a slight reduction in consistency, indicating decreased workability. To achieve the

target consistency, additional mixing water was required for the TiO_2-containing mixtures. This behavior can be attributed to the high specific surface area of TiO_2 particles, which increases water demand and alters the rheological properties of the fresh mortar. Similar findings have been reported by Hatori, Giordani, Casarin, and Guerra (2023) [20], who observed increased water demand and reduced workability in photocatalytic cement-based materials containing TiO_2.

3.2. X-Ray diffraction analysis. Figure 6 presents the X-ray diffraction (XRD) patterns of the mortars containing 0%, 2%, 6%, and 10% TiO_2. The diffractograms reveal the principal crystalline phases present in the cementitious matrix and provide information regarding the mineralogical composition of the mortars after curing. The XRD analysis enables identification of hydration products and mineral constituents derived from the raw materials, as well as crystalline TiO_2 incorporated into the mixtures. Variations in peak intensity among the formulations may be associated with the increasing TiO_2 content and its interaction with the cementitious

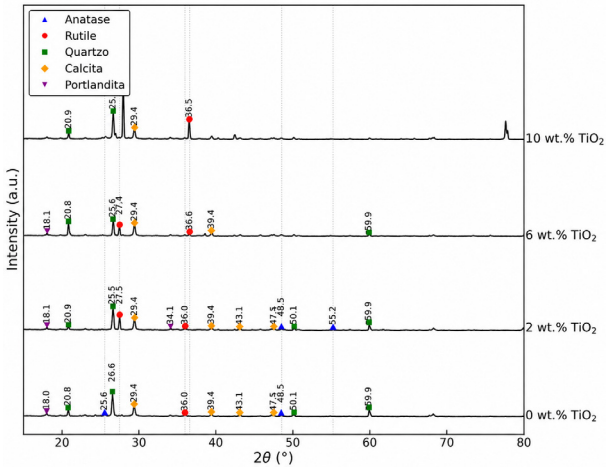

Figure 6. X-ray diffraction patterns of mortars containing 0%, 2%, 6%, and 10% TiO_2.

matrix. A detailed interpretation of the diffraction peaks is presented in the following sections.

For the mortar sample without titanium dioxide addition (0% TiO_2), the X-ray diffraction (XRD) analysis revealed the presence of crystalline phases commonly found in cement-based materials. Silicon dioxide (SiO_2), corresponding to quartz, was identified according to JCPDS reference pattern No. 01-083-2465, 01-085-0335, and 01-087-2096, indicating the presence of siliceous aggregates used in the mortar composition. Calcium carbonate ($CaCO_3$) phases were also detected, as evidenced by JCPDS reference pattern No. 01-081-2027 and 01-072-1937. These phases are typically associated with limestone filler and carbonation products formed during the curing process.

In addition, calcium oxide (CaO) was identified based on JCPDS reference pattern No.00-017-0912, which may be related to residual free lime resulting from incomplete hydration reactions of the cementitious matrix. Heat-activated hydrated cement powder develops new active components such as calcium silicate and calcium oxide, which then participate in further hydration in new mortars; incomplete reaction can leave residual CaO [21]. A phase corresponding to JCPDS reference pattern No. 96-210-1125 (C352.00) was also detected, possibly associated with complex cement hydration products present in the mortar.

Overall, the XRD results indicate that the reference mortar matrix is predominantly composed of quartz and calcium carbonate, which are characteristic phases of conventional rendering mortars. Hydration of Portland cement typically forms calcium silicate hydrate (C–S–H) and related gel phases; these are poorly crystalline but can be associated with specific complex calcium–silicate–hydrate structures in XRD [22]. The absence of diffraction peaks associated with TiO_2 confirms that no photocatalytic additive was incorporated into this formulation, making it an appropriate control sample for comparison with TiO_2-modified mortars in subsequent microstructural and photocatalytic performance analyses.

For the mortar containing 2% TiO_2, diffraction peaks were observed at 2θ values of 27.719°, 36.302°, 39.601°, 44.507°, 54.804°, 57.245°, 64.769°, 66.152°, 70.225°, and 73.170°. These reflections are consistent with the rutile phase of TiO_2, according to the JCPDS reference pattern No. 01-088-1173. Rutile is a thermodynamically stable polymorph of titanium dioxide characterized by a tetragonal crystal structure composed of distorted TiO_6 octahedra, which contribute to its electronic and photocatalytic properties [23, 24].

In addition to the TiO_2-related reflections, diffraction peaks associated with silicon dioxide (SiO_2), calcium carbonate ($CaCO_3$), and calcium titanium silicate ($CaTiSiO_5$, titanite) were also detected. These phases are attributed to the mineral constituents of the aggregate and cementitious matrix, indicating the coexistence of multiple crystalline phases within the mortar.

The mortar containing 6% TiO_2 exhibited diffraction peaks at 2θ values of 25.273°, 36.881°, 37.700°, 38.509°, 47.981°, 54.992°, 68.593°, 70.199°, 73.856°, and 75.939°. These reflections are consistent with the anatase phase of TiO_2, according to the JCPDS reference pattern No. 96-500-0224. Anatase is widely recognized as the most photocatalytically active TiO_2 polymorph due to its high specific surface area and favorable charge-carrier dynamics, which enhance the generation and separation of photogenerated electron–hole pairs [25]. Additional diffraction peaks associated with SiO_2 and calcium oxide (CaO) were also identified, suggesting the presence of mineral phases originating from the aggregate and hydration products formed during cement curing. The coexistence of anatase with these phases reflects the complex mineralogical composition of the mortar matrix.

For the mortar containing 10% TiO_2, diffraction peaks were identified at 2θ values of 27.436°, 36.087°, 39.189°, 56.632°, 64.062°, and 69.798°, which are consistent with the rutile phase of TiO_2 according to JCPDS reference pattern No. 00-034-0180. Additional peaks were attributed to SiO_2, $CaCO_3$, $CaTiSiO_5$ (titanite), and calcium silicate phases, including hatrurite. In TiO_2-modified OPC mortars, peaks for quartz (SiO_2) and calcium silicate (Ca_2SiO_4) are clearly identified and matched with JCPDS cards, with calcium silicate peaks around 26–39° [26]. The identification of both anatase and rutile phases among the TiO_2-modified mortars is particularly relevant because these polymorphs exhibit dis-

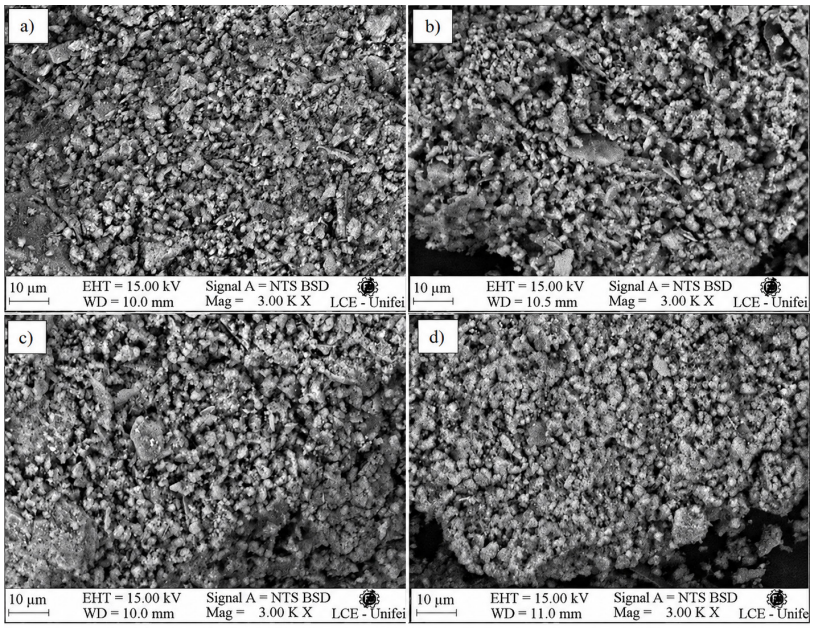

Figure 7. SEM micrographs of mortar samples containing different TiO_2 contents: (a) 0% (reference mortar), (b) 2%, (c) 6%, and (d) 10%, after 28 days of curing.

tinct photocatalytic behaviors. Anatase is generally associated with higher photocatalytic activity owing to its superior charge-carrier mobility and larger specific surface area, whereas rutile may contribute to charge-transfer processes and improve photocatalytic efficiency when present in combination with anatase. Therefore, the crystalline composition revealed by XRD may partially explain the differences observed in methylene blue degradation among the investigated formulations.

3.3. Scanning electron microscopy and energy-dispersive spectroscopy analysis. Figure 7 presents the scanning electron microscopy (SEM) micrographs and energy-dispersive X-ray spectroscopy (EDS) analyses of the reference mortar and the mortars containing 0%, 2%, 6%, and 10% TiO_2 after 28 days of curing.

For the reference mortar (Figure 7a), the SEM images reveal a heterogeneous microstructure composed of particles with different sizes, shapes, and surface textures. At a magnification of 3kx, larger angular particles and smaller irregular particles can be observed dispersed throughout the matrix. Based on the combined SEM, EDS, and XRD results, the angular particles may be associated with calcium-rich phases, including calcium carbonate ($CaCO_3$), whereas the finer particles are consistent with silica-rich constituents originating from the aggregate. Recycled aggregates and modified fines often show granular or angular $CaCO_3$ deposits enriched in Ca, C and O on particle surfaces in SEM–EDS, matching your description of larger angular calcium-rich particles [27].

The differences in particle morphology and surface texture become more evident. Some particles exhibit rough and well-defined surfaces that are consistent with crystalline phases identified by XRD, while other regions display finer and more irregular morphologies. The observed contrast variations are likely related to differences in elemental composition and local density within the cementitious matrix. The EDS spectrum of the reference mortar, shown in Figure 8(a), confirmed the presence of oxygen (O), calcium (Ca), silicon (Si), and carbon (C), indicating the coexistence of calcium-rich and silica-rich phases, including calcium carbonate ($CaCO_3$). In addition, minor concentrations of aluminum (Al), iron (Fe), magnesium (Mg), and potassium (K) were identified. These elements are typically associated with clinker-derived compounds and naturally occurring mineral constituents present in both cement and aggregates.

The SEM micrographs and EDS spectrum of the mortar containing 2% TiO_2, presented in Figure 7(b), compared with the reference mixture, the incorporation of TiO_2 resulted in the appearance of brighter particles and localized agglomerates dispersed within the matrix. According to the XRD results, these features are consistent with the presence of rutile TiO_2. However, direct phase identification based solely on morphology is not possible, and the interpretation was supported by the combined SEM, EDS, and XRD analyses. TiO_2 nanoparticles often agglomerate, and this is highlighted as a key practical issue: their tendency to cluster makes dispersion crucial for effective application in cementitious materials [28, 29]. As shown in Figure 8(b), the EDS spectrum confirmed the presence of titanium (Ti), in addition to Ca, Si, O, and C, corroborating the incorporation of TiO_2 into the mortar. Regions containing simultaneous signals of Ti, Ca, and Si may indicate local interactions between TiO_2 particles and the cementitious matrix, although the formation of specific secondary phases cannot be confirmed solely by EDS analysis.

As shown in Figure 7(c), the mortar containing 6% TiO_2 SEM observations revealed a more uniform distribution of fine particles throughout the matrix compared with the 2% formulation. Fine particulate structures and particle clusters were observed, which are consistent with the presence of TiO_2 identified by XRD as predominantly anatase. As shown in Figure 8(c), The EDS analysis detected significant amounts of Ti, confirming the successful incorporation of

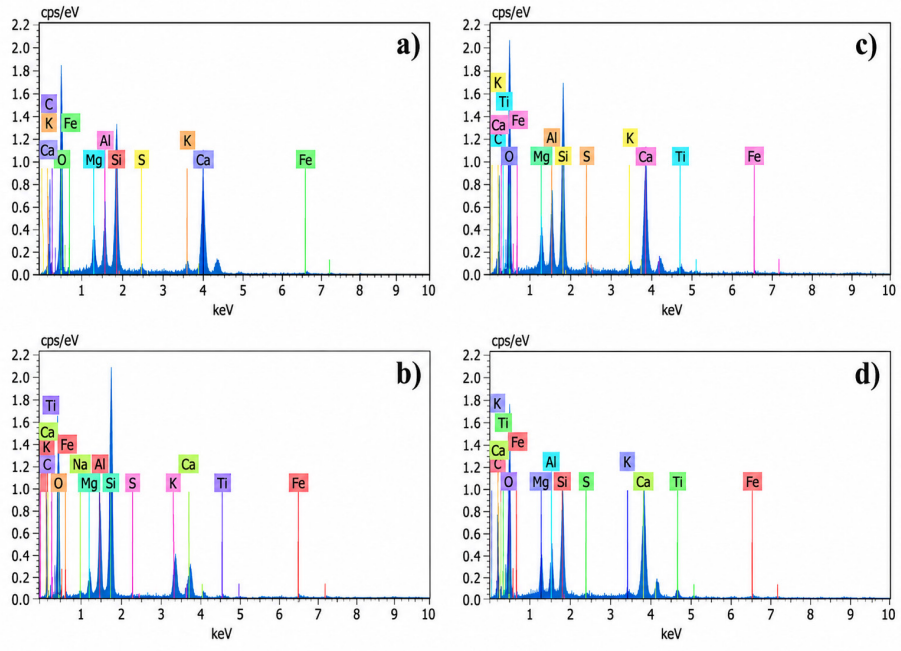

Figure 8. EDS of mortar samples containing different TiO_2 contents: (a) 0% (reference mortar), (b) 2%, (c) 6%, and (d) 10%, after 28 days of curing.

the photocatalyst. The coexistence of Ti, Si, Ca, and O within the analyzed regions indicates the interaction between the photocatalyst and the hydrated cement matrix. The more homogeneous distribution observed in this formulation may contribute to increased exposure of photocatalytic active sites, which is an important factor influencing photocatalytic performance.

As shown in Figure 7(d), the microstructure of the mortar containing 10% TiO_2 revealed a higher concentration of TiO_2-rich particles and the formation of particle agglomerates, these agglomerates suggest that increasing TiO_2 content may reduce dispersion efficiency within the mortar matrix. As shown in Figure 8(d) The EDS analysis identified O, Si, Ca, Ti, Fe, K, Mg, and Al, indicating a complex mineralogical composition consistent with the phases detected by XRD. The presence of Ti-rich regions confirms the incorporation of the photocatalyst, whereas the coexistence of Ca- and Si-rich phases reflects the hydrated cementitious matrix and aggregate constituents.

The observed agglomeration of TiO_2 particles in the 10% mortar is particularly relevant when interpreting the photocatalytic results. Although higher TiO_2 contents increase the amount of photocatalytically active material, excessive particle agglomeration may reduce the effective surface area exposed to ultraviolet radiation and limit the accessibility of active sites. Therefore, photocatalytic performance is influenced not only by TiO_2 concentration but also by its dispersion and distribution within the cementitious matrix [30].

Surface area is a key factor governing the photocatalytic activity of TiO_2-based cementitious materials because it determines the number of active sites available for light absorption and pollutant adsorption. The incorporation of TiO_2 nanoparticles is expected to increase the overall specific surface area of the mortar matrix due to their fine particle size. However, excessive TiO_2 loading may promote particle agglomeration, as observed in the SEM images, thereby reducing the effective exposed surface area and limiting the accessibility of photocatalytically active sites. Therefore, photocatalytic performance depends not only on TiO_2 content but also on the balance between surface area enhancement and particle dispersion within the cementitious matrix.

The photocatalytic efficiency of TiO_2-modified cementitious materials is not solely determined by the amount of TiO_2 added; rather, it is critically influenced by how well the particles are dispersed and distributed within the matrix. While higher TiO_2 content increases the potential for photocatalytic activity, excessive loading often leads to particle agglomeration, which reduces the effective surface area exposed to UV light and limits access to active sites, ultimately diminishing performance [31, 32].

3.4. Photocatalytic activity evaluation by UV–Vis spectroscopy. Figure 9 presents the UV–Vis absorbance spectra of the mortar containing 2% TiO_2 at 10% different exposure times (0, 30, 60, and 90 min) during the photocatalytic test. The analysis was performed over the wavelength range from 400 to 800 nm, covering both the ultraviolet and visible regions. It is important to note that the methylene blue removal observed in this study may result from the combined effects of adsorption by the cementitious matrix and photocatalytic degradation induced by TiO_2 under UV irradiation. Since no adsorption–desorption equilibrium stage was performed before the photocatalytic tests, the reported discoloration efficiencies represent the overall dye removal. Future studies should include dark adsorption experiments to distinguish the individual contributions of adsorption and photocatalysis.

As shown in Figure 9, a gradual decrease in absorbance was observed with increasing irradiation time, particularly in the characteristic absorption region of methylene blue between 600 and 700 nm. This behavior indicates the progressive degradation of the dye mole-

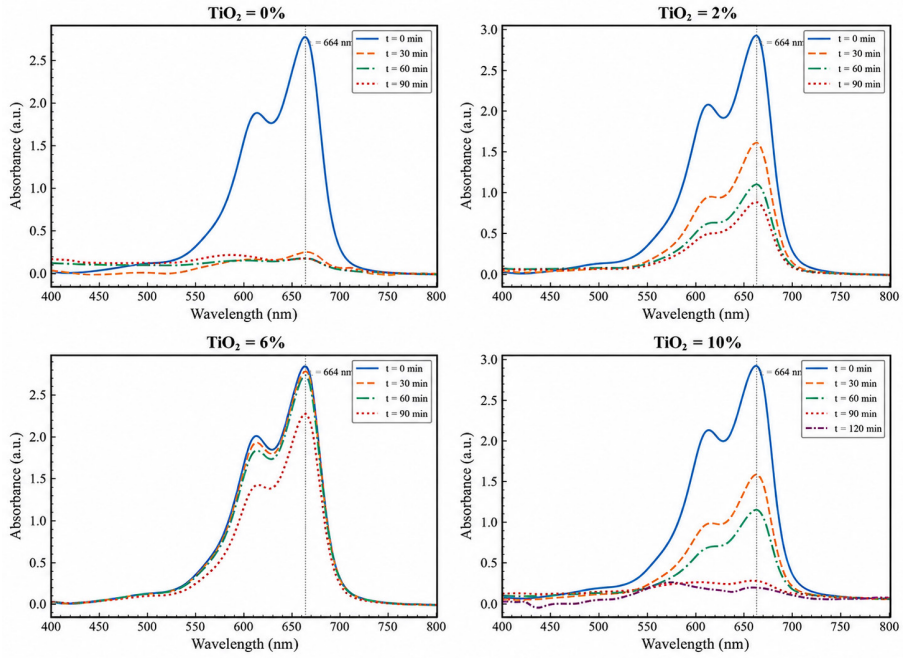

Figure 9. UV–Vis absorbance spectra of methylene blue solution recorded during photocatalytic degradation in the presence of mortar samples containing 2–10% TiO_2.

cules and demonstrates the photocatalytic activity of the TiO_2-modified mortar. The reduction in absorbance intensity over time suggests a decrease in methylene blue concentration as photocatalytic reactions proceed on the mortar surface.

The most pronounced changes occurred within the visible region, where methylene blue exhibits its main absorption band, confirming the effectiveness of the photocatalytic process. The photocatalytic activity of the TiO_2-modified mortars is governed by the semiconducting properties of TiO_2, whose anatase and rutile crystalline phases were confirmed by XRD analysis. TiO_2 is an n-type semiconductor with a band gap of approximately 3.2 eV for anatase and 3.0 eV for rutile [23, 25]. When irradiated with ultraviolet light, photons with energy equal to or greater than the band gap promote electrons from the valence band to the conduction band, generating electron–hole (e^-/h^+) pairs. These charge carriers migrate to the catalyst surface, where photogenerated holes oxidize adsorbed water or hydroxyl groups to produce hydroxyl radicals (•OH), while conduction-band electrons reduce dissolved oxygen to form superoxide radicals ($•O_2^-$) [25, 33]. These reactive oxygen species are responsible for the oxidation and mineralization of methylene blue molecules adsorbed on the mortar surface, resulting in the observed photocatalytic degradation [25, 33, 34].

For the 6% TiO_2 sample, absorbance progressively decreased with increasing irradiation time, particularly in the ultraviolet region near 300 nm and in the visible region between 600 and 700 nm. This behavior indicates the effective photocatalytic degradation of methylene blue molecules, driven by photoinduced reactions occurring at the TiO_2 surface, leading to a reduction in dye concentration over time. According to Dalhat and Ahmad (2022) [34], the photocatalytic efficiency of TiO_2 is associated with the generation of highly reactive species, including hydroxyl radicals (•OH) and reactive oxygen species, which promote the oxidation and decomposition of organic contaminants. The progressive decrease in absorbance observed during the experiment is consistent with these photocatalytic mechanisms. The results indicate that the mortar containing 6% TiO_2 exhibited measurable photocatalytic activity, evidenced by the continuous reduction in methylene blue absorbance throughout the exposure period.

For the 10% TiO_2 sample, the absorbance spectra showed a progressive decline relative to the initial spectrum as the irradiation time increased. This reduction was particularly pronounced in the characteristic absorption band of methylene blue, demonstrating the enhanced photocatalytic activity of the TiO_2-containing material and the effective degradation of dye molecules throughout the irradiation process. This behavior is consistent with the photocatalytic oxidation mechanism of TiO_2, in which reactive species such as hydroxyl radicals (•OH) and reactive oxygen species are generated under UV irradiation and subsequently attack organic molecules adsorbed on the photocatalyst surface [33].

The continuous decrease in absorbance after 60 and 90 min confirms that the photocatalytic process remained active throughout the experimental period. Among the investigated formulations, the mortar containing 10% TiO_2 exhibited the greatest reduction in methylene blue absorbance, indicating superior photocatalytic performance.

As illustrated in Figure 10, photogenerated holes react with adsorbed water molecules or hydroxyl ions to produce hydroxyl radicals (•OH), whereas conduction-band electrons reduce dissolved oxygen to form superoxide radicals ($•O_2^-$). These reactive oxygen species attack the chromophoric structure of methylene blue through successive oxidation reactions, producing intermediate compounds that are subsequently mineralized into CO_2, H_2O, and inorganic ions. Conse-

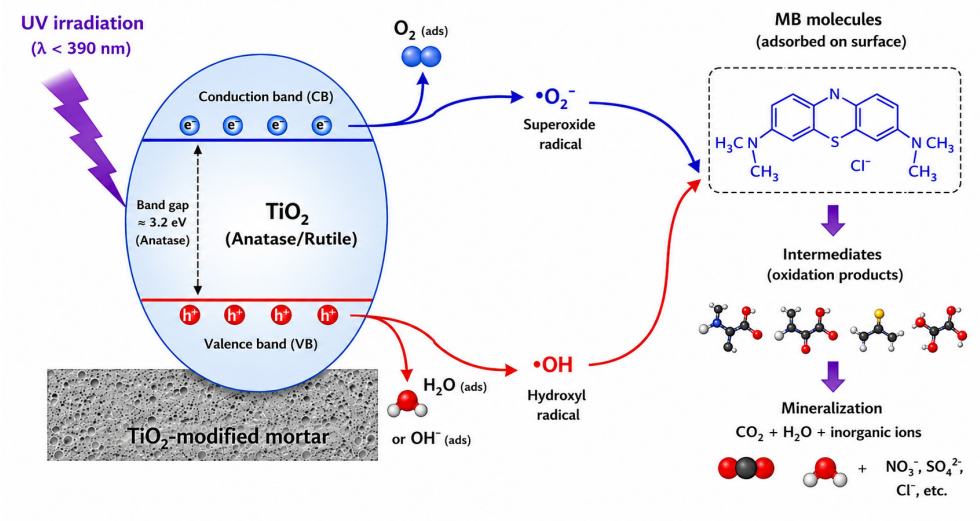

Figure 10. Proposed photocatalytic mechanism for methylene blue (MB) degradation on TiO_2-modified mortar under UV irradiation. Upon UV excitation, TiO_2 generates electron–hole pairs that promote the formation of hydroxyl (•OH) and superoxide ($•O_2^-$) radicals. These reactive oxygen species oxidize methylene blue molecules adsorbed on the mortar surface, leading to intermediate products and, ultimately, mineralization into CO_2, H_2O, and inorganic ions.

quently, the photocatalytic efficiency depends on the effective generation of electron–hole pairs, suppression of charge recombination, and the accessibility of TiO_2 particles exposed at the mortar surface.

Figure 11 summarizes the methylene blue (MB) removal behavior of mortar samples containing different TiO_2 contents (0%, 2%, 6%, and 10%) under UV irradiation. The results are presented as (a) the normalized concentration (C/C_0) as a function of irradiation time, (b) pseudo-first-order kinetic fitting for the TiO_2-containing mortars, (c) the apparent first-order rate constants (k), and (d) a heat map showing the evolution of MB removal efficiency over time.

As shown in Figure 11(a), the reference mortar without TiO_2 (0%) exhibited the fastest decrease in C/C_0, reaching approximately 0.08 after 90 min, corresponding to an overall MB removal of approximately 92%. Among the TiO_2-modified mortars, the formulation containing 10 wt.% TiO_2 showed the greatest decrease in MB concentration, achieving approximately 93% removal after 90 min. The mortar containing 2 wt.% TiO_2 exhibited intermediate behavior, with a final removal efficiency of approximately 70%, whereas the 6 wt.% TiO_2 mortar showed the lowest performance, reaching only about 20% removal.

Since no adsorption–desorption equilibrium was established before UV irradiation, the behavior of the reference mortar cannot be interpreted exclusively in terms of photocatalytic activity. For this reason, the pseudo-first-order kinetic model was applied only to the TiO_2-containing mortars, as shown in Figure 11(b). The rapid MB removal observed for the 0% mortar is mainly attributed to adsorption by the porous cementitious matrix rather than to photocatalytic degradation.

The kinetic analysis revealed apparent first-order rate constants of 0.0171 min^{-1} for the 2 wt.% TiO_2 mortar, 0.0018 min^{-1} for the 6 wt.% TiO_2 mortar, and 0.0172 min^{-1} for the 10 wt.% TiO_2 mortar (Figure 11(c)). The 2 wt.% and 10 wt.% formulations exhibited very similar reaction rates, whereas the 6 wt.% mortar presented a much lower kinetic constant, indicating limited photocatalytic effectiveness. The reduced performance of this formulation may be associated with particle agglomeration, poorer dispersion within the cementitious matrix, or reduced accessibility of photocatalytically active sites, as also suggested by the SEM observations.

The heat map presented in Figure 11(d) provides a clear visualization of the evolution of MB removal efficiency throughout the experiment. The reference mortar exhibited rapid initial removal, reaching more than 90% after 30 min, whereas the TiO_2-modified mortars showed distinct behaviors depending on TiO_2 content. The 10 wt.% mortar displayed the highest removal efficiency among the photocatalytic mortars throughout the experiment, while the 6 wt.% formulation remained at low efficiency levels during the entire irradiation period.

Overall, the results demonstrate that TiO_2 incorporation strongly influences the apparent photocatalytic behavior of the mortars. Among the TiO_2-modified formulations, the mortar containing 10 wt.% TiO_2 exhibited the highest overall MB removal efficiency (93%) and the highest apparent reaction rate constant (k = 0.0172 min^{-1}). However, photocatalytic performance did not increase linearly with TiO_2 content, highlighting the importance of factors such as particle dispersion, agglomeration, and accessibility of active sites.

It is important to emphasize that the similar overall MB removal efficiencies obtained for the reference mortar (92%) and the 10 wt.% TiO_2 mortar (93%) should not be interpreted as equivalent photocatalytic performance. Because no dark adsorption–desorption equilibrium was performed before UV irradiation, the measured discoloration reflects the combined effects of adsorption and photocatalytic degradation. The porous cementitious matrix of the reference mortar can adsorb a substantial fraction of methylene blue, whereas TiO_2 promotes the photocatalytic oxidation of adsorbed molecules through the generation of reactive oxygen species under UV irradiation. Therefore, the purpose of incorporating TiO_2 is not merely to increase dye removal, but to introduce photocatalytic functionality capable of degrading adsorbed organic contaminants rather than simply retaining them. Future studies will include dark adsorption experiments to quantitatively distinguish adsorption from photo-

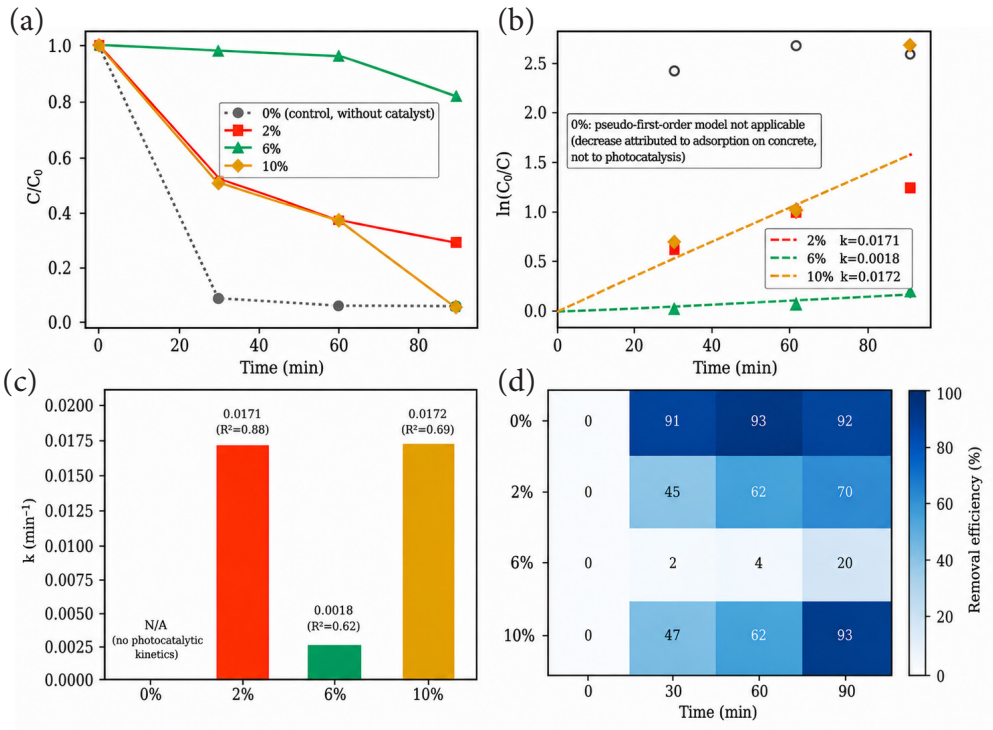

Figure 11. Summarizes the photocatalytic performance of the investigated mortars, (a) degradation (C/C_0), (b) pseudo-first-order kinetic plots (linear fit through the origin for catalyzed samples), (c) rate constant (k), and (d) removal efficiency heat map (%).

Table 3. Comparison of the photocatalytic performance of TiO_2-modified cementitious materials reported in the literature.

Ref.	Material	TiO_2 (wt.%)	Target pollutant	Light source	Irradiation time (min)	Photocatalytic performance	Kinetic parameter	Main finding
[3]	TiO_2 cement slurry	-	NOx	UV	60	Up to 92% NOx removal	Not reported	High NOx abatement
[4]	Rendering mortar + mineral admixtures	-	NO	UV-A	-	Highest NO conversion (MK20)	Not reported	Mineral admixtures enhanced activity
[19]	Nano-TiO_2 recycled aggregate mortar	-	MB (self-cleaning)	UV	2800	51.7% self-cleaning efficiency	Not reported	Improved self-cleaning behavior
[26]	OPC mortar with nano-TiO_2	-	RhB	Solar	-	69.9–84.6% discoloration	Not reported	Surface application more effective
[31]	Rutile TiO_2 mortar	4-6	RhB	Solar	-	Qualitative improvement	Not reported	Optimum under natural sunlight
[32]	Nano-TiO_2 cementitious composite	1	NOx	UV	45	Highest NOx removal	Not reported	Efficiency increased with nano-TiO_2 content
This work	Rendering mortar	10	Methylene blue	UV	120	92% MB removal	k = 0.0172 min^{-1}	Highest MB removal among TiO_2-modified mortar

catalytic degradation. Table 3 summarizes representative studies on TiO_2-modified cementitious materials and compares their photocatalytic performance with that obtained in the present work. A direct quantitative comparison should be interpreted with caution because the reported studies differ considerably in terms of target pollutant (NOx, RhB, or methylene blue), TiO_2 content, irradiation source, exposure time, specimen preparation, and evaluation methodology. Therefore, the comparison is intended to position the proposed mortar within the current state of the art rather than establish a strict performance ranking.

Despite these experimental differences, the results demonstrate that TiO_2 incorporation consistently enhances the photocatalytic functionality of cementitious materials, the mortar containing 10 wt.% TiO_2 developed in this study achieved the highest methylene blue removal among the investigated formulations, reaching approximately 92% removal after 120 min of UV irradiation, with an apparent pseudo-first-order kinetic constant of 0.0172 min^{-1}. These results are consistent with the performance trends reported for other TiO_2-based photocatalytic mortars and confirm the potential of the proposed material for self-cleaning and environmental remediation applications.

4. CONCLUSION

This study investigated the development and characterization of TiO_2-modified rendering mortars, focusing on their structural, microstructural, mineralogical, and photocatalytic behavior under UV irradiation. The combined characterization techniques demonstrated that TiO_2 was successfully incorporated into the cementitious matrix and significantly influenced the MB removal behavior of the investigated mortars.

X-ray diffraction analyses identified both anatase and rutile TiO_2 crystalline phases together with the characteristic mineral phases of the cementitious matrix. SEM/EDS observations revealed that TiO_2 addition modified the mortar microstructure, affecting particle distribution and the formation of localized agglomerates. These microstructural characteristics are consistent with the differences observed in the MB removal behavior among the investigated formulations.

The MB removal experiments showed distinct performances depending on TiO_2 content. Among the TiO_2-modified mortars, the specimens containing 2 wt.% and 10 wt.% TiO_2 achieved overall MB removal efficiencies of approximately 70% and 93%, respectively, after 90 min of UV irradiation, whereas the 6 wt.% TiO_2 mortar exhibited the lowest efficiency (20%). These results indicate that the apparent photocatalytic performance does not increase linearly with TiO_2 content but depends on factors such as particle dispersion, agglomeration, and the accessibility of photocatalytically active sites. Among the photocatalytic mortars, the 10 wt.% TiO_2 formulation exhibited the highest overall MB removal and the highest apparent photocatalytic performance. It should be emphasized that the reference mortar without TiO_2 also exhibited a high MB removal efficiency (approximately 92%). However, because no adsorption–desorption equilibrium was established before UV irradiation, the measured dye removal represents the combined effects of adsorption by the porous cementitious matrix and photocatalytic degradation. Consequently, the high removal efficiency observed for the reference mortar should not be interpreted as evidence of superior photocatalytic activity. Instead, the role of TiO_2 is to promote the photocatalytic oxidation of adsorbed organic molecules through the generation of reactive oxygen species under UV irradiation rather than simply increasing dye adsorption.

Although increasing the TiO_2 content improved the overall performance among the photocatalytic mortars, higher TiO_2 additions also reduced mortar workability owing to the high specific surface area of the nanoparticles, increasing the water demand required to achieve adequate consistency during mixing. T

he developed TiO_2-modified rendering mortars demonstrate potential for application as multifunctional building coatings, particularly for self-cleaning façades and environmentally active surfaces capable of degrading organic contaminants. Nevertheless, the present study also highlights the importance of distinguishing adsorption from photocatalytic degradation when evaluating cement-based photocatalytic materials.

Future work should therefore include adsorption–desorption equilibrium experiments prior to UV irradiation to quantify the individual contributions of adsorption and photocatalysis. In addition, surface-sensitive characterization techniques, such as X-ray Photoelectron Spectroscopy (XPS), quantitative elemental mapping, and Brunauer–Emmett–Teller (BET) specific surface area measurements, should be employed to correlate the amount of exposed TiO_2, particle dispersion, and accessible active sites with photocatalytic performance. Long-term durability and outdoor performance under natural environmental conditions should also be investigated

ACKNOWLEDGEMENTS

The authors would like to express their gratitude for the financial support from the Minas Gerais Research Foundation (FAPEMIG– Grant APQ-03495).

CREDIT AUTHOR STATEMENT

Vander Alkmin dos Santos Ribeiro: Investigation, Data curation, Formal analysis, Writing-original draft preparation, Methodology, Writing-original draft preparation, Conceptualization. **Adhimar Flávio Oliveira:** Investigation, Data curation, Formal analysis, Writing-original draft preparation, Methodology, Supervision, Writing-original draft preparation, Conceptualization. **Celso Henrique Correa Carvalho:** Methodology, Investigation, Data curation, Formal analysis. **Lucas Pacca e Silva:** Methodology, Data curation, Data curation.

DECLARATIONS

Conflict of interest The authors declare that they have no known competing financial interests or personal relationships that could have appeared to influence the work reported in this paper.

AVAILABILITY OF DATA

All data supporting the findings of this study are included within the manuscript. Any additional data related to this work is available from the corresponding author upon reasonable request.

AI DISCLOSURE STATEMENT

The authors declare that no Generative AI tools were used in the preparation, writing, analysis, or editing of this manuscript.

REFERENCES

[1] Kotzias, D. 2024. "Photo-Induced Degradation of Priority Air Pollutants on TiO_2-Based Coatings in Indoor and Outdoor Environments—A Mechanistic View of the Processes at the Air/Catalyst Interface." Crystals 14. https://doi.org/10.3390/cryst14070661.

[2] Bersch, J. D., I. Flores-Colen, A. B. Masuero, and D. C. C. Dal Molin. 2023. "Photocatalytic TiO_2-Based Coatings for Mortars on Facades: A Review of Efficiency, Durability, and Sustainability." Buildings 13. https://doi.org/10.3390/buildings13010186.

[3] Jabali, Y., J. Assaad, and G. Aouad. 2023. "Photocatalytic Activity and Mechanical Properties of Cement Slurries Containing Titanium Dioxide." Buildings 13. https://doi.org/10.3390/buildings13041046.

[4] Lara, R. C., G. C. Xavier, M. C. Canela, J. A. Carvalho, J. Alexandre, and A. R. G. Azevedo. 2023. "Characterization and Photocatalytic Performance of Cement Mortars with Incorporation of TiO_2 and Mineral Admixtures." Environmental Science and Pollution Research 30: 95537–95549. https://doi.org/10.1007/s11356-023-29084-6.

[5] Sadia, S. I., M. K. H. Shishir, S. Ahmed, A. R. Aidid, M. M. Islam, M. M. Rana, S. M. Al-Reza, and M. A. Alam. 2024. "Crystallographic Biography on Nanocrystalline Phase of Polymorphs Titanium Dioxide (TiO_2): A Perspective Static Review." South African Journal of Chemical Engineering 50: 51–64. https://doi.org/10.1016/j.sajce.2024.07.005.

[6] Lal, M., P. Sharma, and C. Ram. 2022. "Synthesis and Photocatalytic Potential of Nd-Doped TiO_2 under UV and Solar Light Irradiation Using a Sol-Gel Ultrasonication Method." Results in Materials 15: 100308. https://doi.org/10.1016/j.rinma.2022.100308.

[7] Janczarek, M., Ł. Klapiszewski, P. Jędrzejczak, I. Klapiszewska, A. Ślosarczyk, and T. Jesionowski. 2022. "Progress of Functionalized TiO_2-Based Nanomaterials in the Construction Industry: A Comprehensive Review." Chemical Engineering Journal 430: 132062. https://doi.org/10.1016/j.cej.2021.132062.

[8] Nisar, M.; Khan, N.; Qadir, M.I.; Shah, Z. 2025. "Recent Advances in TiO_2 -Based Photocatalysts for Efficient Water Splitting to Hydrogen." Nanomaterials 15: 984. https://doi.org/10.3390/nano15130984.

[9] ABNT NBR 7175. 2003. "Cal Hidratada para Argamassas — Determinação da Plasticidade." Associação Brasileira de Normas Técnicas 2021.

[10] ABNT NBR 16697. 2018. "Cimento Portland — Requisitos." Associação Brasileira de Normas Técnicas.

[11] ABNT NBR 16916. 2021. "Agregado Miúdo — Determinação da Massa Específica e Massa Específica Aparente." Rio de Janeiro.

[12] ABNT NBR 16605. 2017. "Cimento Portland e Outros Materiais em Pó — Determinação da Massa Específica." Rio de Janeiro.

[13] ABNT NBR 13279. 1995. "Argamassa para Assentamento e Revestimento de Paredes e Tetos — Determinação da Retenção de Água." Associação Brasileira de Normas Técnicas.

[14] ABNT NBR 13749. 2013. "Revestimento de Paredes e Tetos de Argamassas Inorgânicas — Especificação." Associação Brasileira de Normas Técnicas.

[15] Carvalho, C. F., A. F. Oliveira, M. E. Leyva Gonzalez, V. Alkmin, C. H. Carvalho, and C. Carvalho. 2026. "Degradation of Organic Pollutants in Water Treatment." journal Applied Materials and technology 7: 74–84 https://doi.org/10.31258/Jamt.7.2.74-84.

[16] Pinton, J. H. B., A. F. Oliveira, D. R. Huanca, and N. D. S. Mohallem. 2024. "Development of an Automated and Cost-Effective Apparatus for Sol-Gel Solution Deposition Using Spray Coating Technique and Its Application for TiO_2-Based Photocatalytic Films." Materials Chemistry and Physics 318: 129213. https://doi.org/10.1016/j.matchemphys.2024.129213.

[17] Pinton, J. H. B., C. H. C. Carvalho, D. R. Huanca, A. M. C. Gomes, N. D. S. Mohallem, and A. F. Oliveira. 2025. "Optimization and Stability of Spray-Coated Titanium Dioxide Thin Films: Influence of Calcination on Photocatalytic Properties for Pollutant Treatment." Journal of Electronic Materials 54: 7914–7926. https://doi.org/10.1007/s11664-025-12108-x.

[18] ABNT NBR 7211. 2022. "Agregados para Concreto — Requisitos." Associação Brasileira de Normas Técnicas.

[19] Zhang, X., W. Chen, W. Lin, J. Zheng, G. Yan, and X. Chen. 2024. "Enhanced Photocatalytic Activity in Photocatalytic Concrete: Synthesis, Characterization, and Comprehensive Performance Assessment of Nano-TiO_2-Modified Recycled Aggregates." Catalysts 14. https://doi.org/10.3390/catal14100711.

[20] Hatori, A., C. Giordani, R. P. Casarin, F. L. Guerra, and A. B. Masuero. 2023. "Avaliação das Propriedades Mecânicas e de Absorção de Água de Argamassas com Adição de Dióxido de Titânio." In XIV Simpósio Brasileiro de Tecnologia das Argamassas (SBTA), 12:9.

[21] Ma, Z., J. Shen, H. Wu, and P. Zhang. 2022. "Properties and Activation Modification of Eco-Friendly Cementitious Materials Incorporating High-Volume Hydrated Cement Powder from Construction Waste." Construction and Building Materials 316: 125788. https://doi.org/10.1016/j.conbuildmat.2021.125788.

[22] Altunci, Y. T., and C. Öcal. 2025. "Assessment of Time-Dependent Hydration Products in Olivine-Substituted Cement Mortars." Materials 18: 1–21. https://doi.org/10.3390/ma18174212.

[23] Eddy, D. R., M. D. Permana, L. K. Sakti, A. N. Sheha, Solihudin, S. Hidayat, T. Takei, N. Kumada, and I. Rahayu. 2023. "Heterophase Polymorph of TiO_2 (Anatase, Rutile, Brookite, TiO_2(B)) for Efficient Photocatalyst: Fabrication and Activity." Nanomaterials 13. https://doi.org/10.3390/

nano13040704.

[24] Geldasa, F. T., and F. B. Dejene. 2025. "Effects of S Doping and Oxygen Vacancy on the Physical Properties of Rutile TiO_2 for Photocatalysis Applications Based on Density Functional Theory Study." Materials 18. https://doi.org/10.3390/ma18081688.

[25] Navidpour, A. H., S. Abbasi, D. Li, A. Mojiri, and J. L. Zhou. 2023. "Investigation of Advanced Oxidation Process in the Presence of TiO_2 Semiconductor as Photocatalyst: Property, Principle, Kinetic Analysis, and Photocatalytic Activity." Catalysts 13. https://doi.org/10.3390/catal13020232.

[26] Reddy, N. A., and P. S. Chandana. 2024. "Microstructural Analysis and Densification of Ordinary Portland Cement Mortars Incorporated with Minimal Nano-TiO_2: Intermixing and Surface Coating on Both Fresh and Hardened Surfaces." Discover Materials 4. https://doi.org/10.1007/s43939-024-00096-4.

[27] Li, X., C. Tian, M. Li, Q. Zhan, X. Wang, and W. Dong. 2025. "Study on the Performance Enhancement of Recycled Fine Aggregate Through Carbonation with Calcium Source Supplied by Industrial Waste Residue." Materials 18. https://doi.org/10.3390/ma18071589.

[28] Choi, Y. 2024. "Degree of Hydration, Microstructure, and Mechanical Properties of Cement-Modified TiO_2 Nanoparticles." Materials 17. https://doi.org/10.3390/ma17184541.

[29] Rachmaniar, S., D. A. Nugraha, D. Santjojo, R. Tjahjanto, N. Mufti, and Masruroh. 2024. "Prevention of Particle Agglomeration in Sol–Gel Synthesis of TiO_2 Nanoparticles via Addition of Surfactant." Journal of Nanoparticle Research 26. https://doi.org/10.1007/s11051-024-05943-2.

[30] Chilmon, K., M. Kalinowski, and W. Jackiewicz-Rek. 2024. "Influence of Coarse Aggregate Exposure on Air Purification Efficiency in Photocatalytic Cement Composites." Buildings. https://doi.org/10.3390/buildings14113639.

[31] Palanisamy, C., G. Parvathikumar, S. Gnanasekaran, S. Jerold, S. Chelladurai, S. Sivananthan, B. Adhavan, N. Geetha, R. Arthanari, and S. Tibebu. 2023. "Study on the Behavior of Self-Cleaning Impregnated Photocatalyst (TiO_2) with Cement Mortar." Advances in Materials Science and Engineering. https://doi.org/10.1155/2023/3571526.

[32] Zhang, X., and X. Chen. 2025. "Eco-Efficient Mortars with High-Content Construction Waste-Derived Aggregates Functionalized via Nano-TiO_2 for NOx Abatement." Processes. https://doi.org/10.3390/pr13061944.

[33] Kong, E. D. H., C. W. Lai, J. Juan, Y. Pang, C. Khe, I. Badruddin, F. Gapsari, and K. Anam. 2025. "Recent Advances in Titanium Dioxide Bio-Derived Carbon Photocatalysts for Organic Pollutant Degradation in Wastewater." iScience 28. https://doi.org/10.1016/j.isci.2025.112368.

[34] Dalhat, M. H., and A. Ahmad. 2022. "Removal of Pesticides from Water and Wastewater by Solar-Driven Photocatalysis." In Development in Wastewater Treatment Research and Processes, edited by M. Shah, S. Rodriguez-Couto, and J. Biswas, 435–458. Elsevier. https://doi.org/10.1016/B978-0-323-85583-9.00012-0.